

Microstructure and Hardness Properties of 304L Stainless Steel at Varied Gas Tungsten Arc Welding Voltage

*¹Bolarinwa J. Kutelu, ²Akinlabi Oyetunji, ²Daniel T. Oloruntoba, ¹Dada O. Omoyeni

¹Department of Mineral and Petroleum Resources Engineering Technology, The Federal Polytechnic, Ado-Ekiti, Ekiti State, Nigeria.

²Department of Metallurgical and Materials Engineering, The Federal University of Technology, Akure, Ondo State, Nigeria

rinwa2006@yahoo.com | laoyetunji@futa.edu.ng | dtoloruntoba@futa.edu.ng | ludarekanmi@gmail.com

Received: 08-JULY-2024; Reviewed: 04-SEP-2024; Accepted: 09-SEP-2024

<https://dx.doi.org/10.4314/fuoyejet.v9i3.21>

ORIGINAL RESEARCH

Abstract: Establishing optimum range of welding parameters requirements is a sine-quo-non for obtaining weldments with the desired microstructure and mechanical properties. Therefore, in this study efforts were made to investigate the effects of varied gas tungsten arc welding voltage on the microstructure characteristics and hardness property of 304L austenitic stainless steel (ASS). To this end, chemical compositions of the as-received 304L ASS plate was determined by Optical emission spectrometry (AR 4 30 metal analyzer). Weldments with butt-joints configuration were produced, using gas tungsten arc welding (GTAW) at 10 V, 20 V, 30 V and 40 V. Microstructures of the weldments were examined, using metallurgical microscope (OMM) (Olympus GX51), and the weldment were tested on Vickers microhardness testing machine. From the results obtained, chemical compositions of the as-received 304L plate revealed 18.325 wt. % s chromium and 8.469 wt.% nickel, adding up to 26.794 wt.% of the total elemental content. The microstructures of the weldments are heterogeneous (non-equilibrium), austenite (γ) and ferrite (δ) are the major phases. γ is the leading phase, while α grains are found within the γ matrix. Grains of the fusion zone (FZ) microstructures are finer as compared to those of the corresponding heat-affected zone (HAZ). Microstructures of both FZ and HAZ are characterized by δ -ferrite, precipitations, inclusions and dendrites of varied numbers and sizes. Hardness values of weldments were high in the range (20 – 25 V) relative to (30 – 40V). And optimum hardness values 205.8VHN and 192.0VHN were revealed by the FZ and HAZ respectively at the GTAW of 20 V, while least hardness values of 201.4VHN and 188.8VHN were revealed by the FZ and HAZ respectively, at GTAW of 40 V

Keywords: dendrites, heterogeneous, inclusion, microstructure characteristic, weldments, δ -ferrite

<https://dx.doi.org/10.4314/fuoyejet.v9i3.21>

1 INTRODUCTION

Increasing use of 304L ASS for industrial purposes, especially in applications, requiring corrosive (salt, alkaline and acid) environments is not unconnected with its excellent corrosion resistance and good weldability (Aamir *et al.*, 2017; Oyetunji, *et al.*, 2013; Woel-Shyan, *et al.*, 2005; Halil Ibrahim and Ramazan, 2003). The Gas tungsten arc welding GTAW process is a popular welding route for applications, requiring precision welding such as obtained in oil and gas industry, chemical industry, sugar processing industry, boiler and nuclear plants (Amer *et al.*, 2015; Devakumar and Jabaraj, 2014; Zakaria *et al.*, 2010). It provides excellent control of heat input, ease of maneuverability and better economy, and it has proven to produce high-quality and superior welds with low penetration in metal alloys as compared to the other competitive arc welding techniques such as shielded metal arc welding (SAW), submerged arc welding (SAW), plasma arc welding (PAW) and gas tungsten arc welding (GTAW) (Laura *et al.*, 2019; Kutelu *et al.*, 2018). However, the weld undergoes localized

heating, leading to non-uniform temperature distribution with concomitant structural and metallurgical changes along the joint (Mohd *et al.*, 2014; Arivarasu *et al.*, 2015 Oyetunji, *et al.*, 2013; Hussain 2010), and as a result of microstructure characteristics and mechanical properties differentials that existed between the parent metal and weld metal, the subject of welds' performance integrity has continue to attract the researchers' interests.

Wichan and Loeshpahn, (2013) investigated effects of low, medium and high GTA welding speed on microstructures, mechanical properties and corrosion behavior of AISI 201 stainless steel sheets, and reported that weld joint with high welding speed exhibited smaller weld bead size, higher tensile strength and elongation, higher hardness and higher pitting corrosion potentials relative to the ones with medium and low welding speeds respectively. Mohamed *et al.* (2024) influence of current welding current on mechanical properties and microstructure of argon arc welding of type-304L austenitic stainless steel, 140 A, 160 A and 180 A currents were used to produce samples F1, F2 and F3 samples, and reported that tensile strength and elongation values of sample F3 were greater than those of F1 and F2, and with increasing welding current, hardness of the samples were reduced. Hardness values of F1, F2 and F3 were 92, 88 and 84 HRB correspondingly. Ahmed *et al.*, (2023) investigated effect of GTAW welding current on the quality of 304L austenitic stainless steel using ER316L. Pipe TP304L with thickness 3 mm and 5 mm was used for the investigation

*Corresponding Author

Section D- MATERIALS AND METARLLUGY/CHEMICAL SCIENCES & RELATED SCIENCE

Can be cited as:

Kutelu B. J., Oyetunji A., Oloruntoba D. T. and Omoyeni D.O. (2024). Microstructure and Hardness Properties of 304L Stainless Steel at Varied Gas Tungsten Arc Welding Voltage FUOYE Journal of Engineering and Technology (FUOYEJET), 9(3), 503-508.

and the samples were welded at 75 A, 105 A and 135 A. They reported that the strength of the weld metals were higher than the base metal, and highest tensile strength for the samples with 3 mm and 5 mm thickness was revealed at the current of 105 A, the microstructures were characterized by ferrite and austenite phases, and microhardness of the weld zone was lower as compared to the heat affected zone (HAZ) and parent metal (PM).

Okonji *et al.* (2019) investigated effect of welding current on the hardness of austenitic stainless steel weld joints, and reported that marginal difference existed in hardness values of the weld metal and base metal at all the welding current used, however there hardness values of the weld metal was reduced with increasing welding current. Ogundimu *et al.* (2019) studied effect of welding current on mechanical properties and microstructure of TIG welding of type-304L austenitic stainless steel plate, thickness of the plate was 6 mm, and it was welded at 150 A, and 170 A to produce samples F3 and F4 respectively. Tensile strength and elongation values of sample F4 were approximately 584 MPa and 19.3% respectively, and were reportedly superior to the corresponding values of F3. While the average microhardness values of 235.7 Hv and 233.4 Hv were obtained for samples F4 and F3 respectively, and hence sample F4 gave the optimum welding current.

Even, though it is well recognized that proper selection of welding parameters is one of the metallurgical approaches for ensuring high quality welds with minimum distortion, it is obvious from the above details that research attention on effect of GTAW voltage is still very scanty in learned journals relative to current and speed. As a result, efforts were made in this study to produce butt joint samples of 304L ASS plate via GTAW technique at varied range of voltage, this is with the aim of obtaining optimum welding voltage.

2 MATERIALS AND METHOD

2.1 MATERIALS

304L austenitic stainless steel plate of length 120 mm, breadth 20 mm and thickness 8 mm was used for the investigation. Other materials were ER 308L filler rod (grade 1.4316), with diameter of 3 mm, non – consumable tungsten electrode and argon gas of 99.8% purity. The equipment used for are optical emission spectrometer (OES), gas tungsten arc welding machine, grinding /polishing machine, optical metallurgical microscope (OMM) and Vickers micro hardness tester.

2.2 METHODS

2.2.1 CHEMICAL COMPOSITION OF THE 304L ASS AND FILLER METAL

Chemical composition of the as-received 304L ASS plate was determined, using optical emission spectrometry (AR 4 30 metal analyzer). The sample was ground, mounted on the sparking point of the spectrometer and sparked

three (3) times. Mean value of the detected elements was recorded. Shown Table 1 and Table 2 are the chemical compositions of the experimental 304L ASS and the 308L filler metal respectively.

Table 1: Chemical composition of the 304L ASS Plate

Element	Wt. %		
C	0.026	Nb	0.009
Si	0.511	Al	0.018
Mn	1.311	Cl	0.002
S	<0.001	Mo	0.069
P	0.013	V	0.083
Cr	18.325	Ti	0.036
Ni	8.469	Fe	75.916
Cu	0.135		

Table 2. Chemical composition of the filler metal

Element	Wt. %
C	<0.03
Si	0.65
Mn	1.65
S	0.03
P	0.03
Cr	19.5-22.0
Ni	9.0-11.0

2.2.2 SAMPLE PREPARATION AND GAS TUNGSTEN ARC WELDING PROCESS

Twenty (20) samples with dimensions of 50 mm x 30 mm x 4.5 mm thickness were cut from the as– received 304L ASS plate with a simple hacksaw. Butt joint weld configuration, comprising of single-V geometry with angle 60° within its edges and root opening of 2.5 mm was used, the root opening was intentionally introduced to allow for sufficient root penetration (Amer *et al.*, 2015). The gas tungsten arc welding machine used is a manually operated welding machine (Clarke TIG 270) with adjustable current and voltage. Prior welding, two pairs of the single-V samples were positioned with respect to each other, aligned accurately, tacked sparingly and welded, using a range of voltage (20V, 25V, 30V, 35V and 40V) at constant speed and current as depicted in summary of the procedure in Table 3. These selected range voltages are within the optimum range earlier adopted by the past researchers (Amer *et al.*, 2015; Oyetunji *et al.*, 2013). The workpiece was fed with filler rod during welding and flow rate of the shielding gas (argon) was 1.5 litres per minute. The weldments were produced following ASTM A778/778M (2016). Fig. 1 is a sample of the produced weldments, indicating the base metal (BM), fusion zone (FZ) and heat affected zone (HAZ).

Table 3. Summary of weldments production procedure

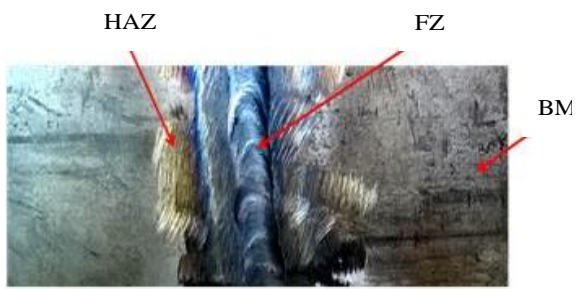


Fig. 1. Butt – joint sample of the weldment

2.2.3 OPTICAL MICROSCOPY

The metallographic samples were prepared in accordance with ASTM E3 – 11 (2011). Conventional metallographic grinding and polishing techniques were used to achieved the desired surface finish. The samples were etched in solution of 50 ml HCl + 50 ml HNO₃ + 50 ml water for two minutes. FZ and HAZ microstructures were viewed and captured by optical metallurgical microscope (OMM) (Olympus GX51) with camera attached.

2.2.4 HARDNESS TEST

Samples used for the microhardness test were prepared in accordance with ASTM E 8 – 04 (2011) standard. They were machined to 20 mm length, 20 mm breadth and 4.5 mm thickness. Vickers micro hardness tester LECO 700AT with diamond pyramid was used for the test. The tests were performed on the transverse cross-section of base metal (BM), heat affected zone (HAZ), fusion zone (FZ) with residence time of 10 seconds. Three indentations were made with gap of about 3 mm in-between on each of the zones (Oyetunji *et al.*, 2013; Halil Ibrahim *et al.*, 2003). Depicted in Fig. 2 shows is the micro hardness test sample.

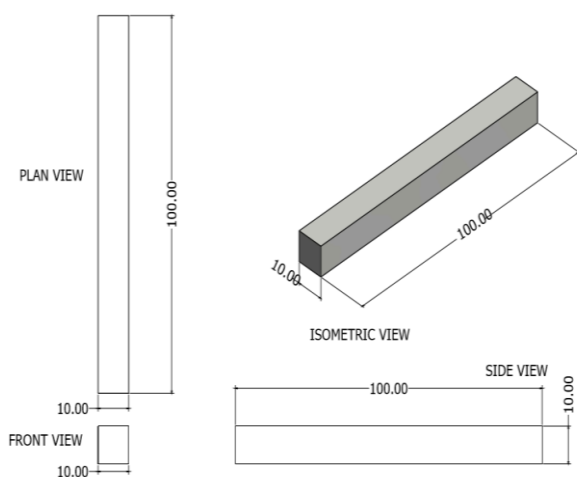


Fig. 2. Hardness test specimen

3 RESULTS AND DISCUSSION

3.1 CHEMICAL COMPOSITION OF THE EXPERIMENTAL

S/No.	Varied parameter Voltage (V)	Parameters held constant	
		Speed (mm/s)	Current (A)
1.	20	4.6	160
2.	25	4.6	160
3.	30	4.6	160
4.	35	4.6	160
5.	40	4.6	160

ASS PLATE

From the result of chemical composition of the as-received shown in Table 1, chromium content of 18.325 wt. % and nickel content of 8.469 wt. % added up to 26.794 wt. % of the total elemental content, making the experimental steel austenitic (Vinoth *et al.*, 2015; Kožuh *et al.*, 2009). And the presence of nickel up to 8.469 wt.% is indicative that the sample is fully austenitic (Arpita *et al.*, 2016). Titanium and niobium prevent carbide formation, and hence their presence up to 0.036 wt. %) and 0.009 wt. % respectively could have enhanced weldability of the ASS plate (Hayes *et al.*, 2006), and the presence of molybdenum up to 0.069 wt. % may enhance resistance of the plate to localized corrosion (Hayes *et al.*, 2006). Chemical composition of the filler metal depicted in Table 2 is similar to chemical composition of the plate. It was carefully selected in order to prevent incident of galvanic corrosion that is often associated with wide compositional differences between workpiece and filler metal (Hayes *et al.*, 2006).

3.2 MICROSTRUCTURES

Plate 1(A–E) are microstructures of the weldments that were produce at 20V, 25V, 30V and 40V respectively. The microstructures are heterogeneous (non-equilibrium), austenite (γ) and ferrite (α) are the major phases. γ is the leading phase, while α grains are found within the γ matrix. In general, grains of the fusion zone (FZ) microstructures are finer as compared to those of the corresponding heat-affected zone (HAZ) microstructures. Microstructures of both FZ and HAZ are characterized by δ -ferrite, precipitations, inclusions and dendrites of varied numbers and sizes.

The GTAW is a heat intensive process, and weld cooling conditions are governed by heat input (Devakumar and Jabaraj, 2014; Ghusoon *et al.*, 2017). Therefore, variations in microstructural features of the sample at the varied welding voltage can be attributed to difference in heat inputs and resulting cooling conditions of the solidification process. Grains of FZs and HAZs microstructures are coarser in the range of 30– 40V as compared to 20 – 25V. The former was due to slow and fast cooling conditions of the solidification process, during which sufficient time was provided for the grains to grow, while the later was due to fast cooling that resulted in grain growth suppression (Kondapalli *et al.*, 2011; Calik, 2009). The different numbers and sizes of dendrites and

inter-dendritic spacing, characterizing FZs and HAZs growth that resulted during welds solidification process. microstructures may partly be attributed to accompanied And from Hall – Petch relationship, coarse grains are temperature gradients of the GTAW process, during which characterized by poor hardness property, while fine there was decrease in subsequent cooling rates with grains by good hardness property (Behnam *et al.*, 2019; increasing distance from the fusion boundary (Arivarasu *et al.*, Hassen, 2005), (Hassen, 2004). The relative low 2015; Gigović-Gekić *et al.*, 2011). In addition, the generated microhardness values of the HAZs may be attributed to chemical gradients of the GTAW process was contributory migration of hardness enhancing elements (C and Mo) (Kožuh *et al.*, 2009).

The increased presence of inclusions in the range (30–40V) as compared to (20–25V) was due to higher heat inputs of the GTAW process (Bhatti *et al.*, 1984), and in congruence, Thewlis and Milner, (1977) attributed the formation of a single phase inclusion - (MnO – SiO₂ – Al₂O₃) at the weld pool that resulted from the combination of oxygen with Mn, Si and Al to high heat input of the welding process.

from HAZ to the FZ or/and BM during the HAZ thermal cycling (Kožuh *et al.*, 2009). In addition, increased migration and displacement of atoms on both sides of grain boundaries, grain boundary mobility and fusion in HAZs were contributory (Arivarasu *et al.*, 2015).

Also, during the thermal cycling of the HAZs, every position experienced a unique thermal change relative to the fusion line, leading to complex mix microstructures, including long dendrites and wide inter dendritic spacing, which may have contributed to therefore low microhardness values of the HAZs may be due to the low microhardness values of the HAZs (Arivarasu *et al.*, 2015; Ahmed *et al.*, 2010). On the other hand, the relative high microhardness values of FZs was due to presence of carbon particles within the γ - α grain. Trapping of the carbon particles within the γ - α grain was possible due to fast cooling conditions of the welds solidification. As a result, there was insufficient time to move away the carbon particles that were in front of γ - α interface (Wan Shaiful *et al.*, 2015; Amer *et al.*, 2015; Gigović-Gekić and Gojić, 2011).

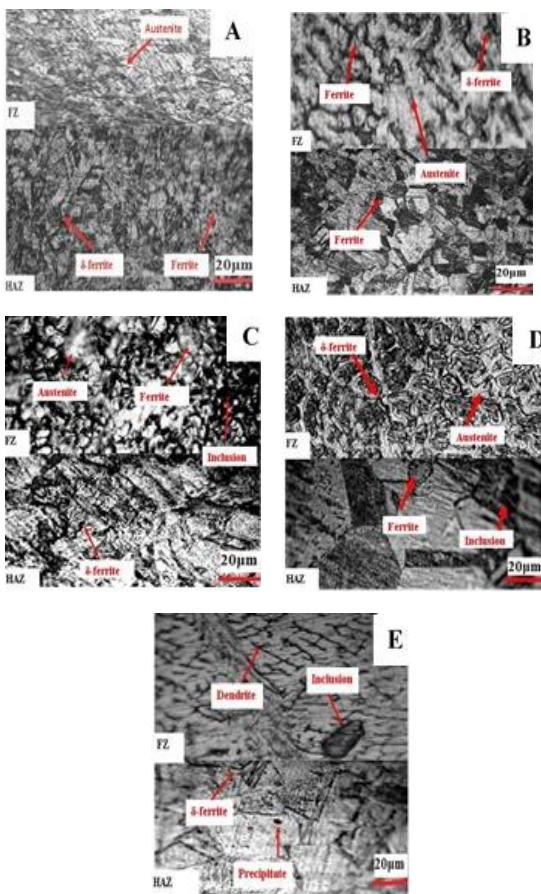


Plate1. (A-E). Optical micrographs of the weldments at GTAW of 20V, 25V, 30V and 40V respectively, etched in solution of 50 ml HCl + 50 ml HNO₃ + 50 ml, and at x400.

3.3 HARDNESS PROPERTY

Fig. 3 and Fig. 4 are microhardness characteristics and map of the weldments respectively, the revealed high microhardness values in the range (20 – 25V) may be attributed to fine grains, and hence grain growth suppression that resulted from fast cooling conditions during welds solidification process. On the other hand, the low microhardness values in the range (30 – 40V) resulted from slow cooling conditions, and hence grain

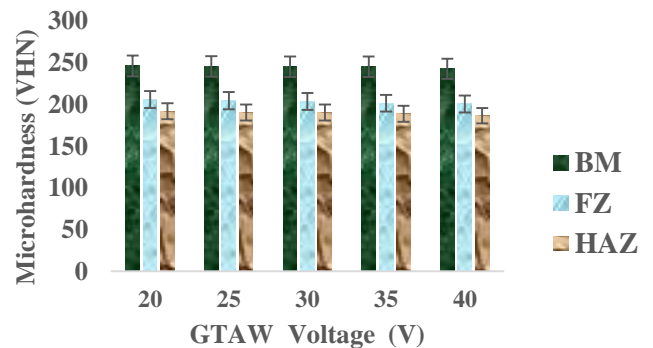


Fig. 3. Microhardness characteristics of the weldment at varied GTAW voltage

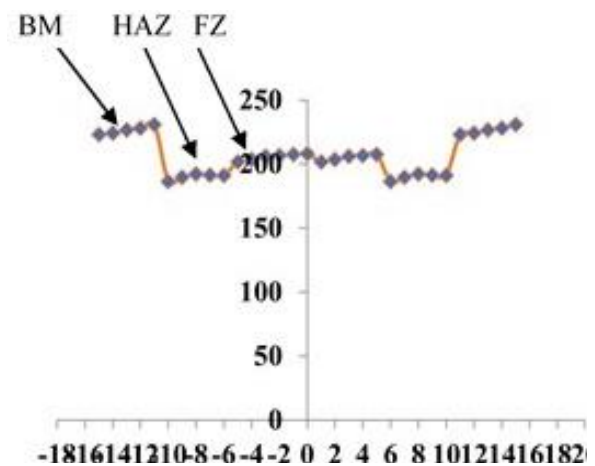


Fig. 4. Microhardness map of the weldment at

varied GTAW voltage

4 Conclusions

From the results of the research, the following conclusions were drawn:

1. Chemical compositions of the as-received 304L plate revealed 18.325 wt. % chromium and 8.469 wt. % nickel, adding up to 26.794 wt. % of the total elemental content.
2. The microstructures of the weldments are heterogeneous (non-equilibrium), austenite (γ) and ferrite (α) are the major phases. γ is the leading phase, while α grains are found within the γ matrix. Grains of the fusion zone (FZ) microstructures are finer as compared to those of the corresponding heat-affected zone (HAZ).
3. Microstructures of both FZ and HAZ are characterized by δ -ferrite, precipitations, inclusions and dendrites of varied numbers and sizes.
4. Hardness values of weldments were high in the range (20 – 25 V) relative to (30 – 40V).
5. Optimum hardness values 205.8VHN and 192.0VHN were revealed by the FZ and HAZ respectively, at the GTAW of 20 V, while least hardness values of 201.4VHN and 188.8VHN were revealed by the FZ and HAZ respectively at GTAW of 40 V, indicating that optimum microstructural characteristics and hence, hardness property was obtained with decreasing GTAW voltage.

REFERENCES

- Aamir, S., Abdul Aziz, M. I., Osama Junaid, M. & Sagheer, A. (2017). Effect of TIG welding parameters on the properties of 304L automated girth welded pipes using orbital welding, *Journal of Material Science*, 136-148.
- Ahmed, H., Imam, E. & Mohamed, R. E. (2023). Effect of GTAW welding current on the quality of 304L austenitic stainless steel using ER316L, *International Journal of Material Technology and Innovation*, 3(2), 10-18, <https://ijmti.journal.ekb.eg/>
- Ahmed, K. H., Abdul, L., Mohd, J. & Pramesh. T. (2010). Influence of welding speed on tensile strength of welded joint in TIG welding process, *International Journal of Applied Engineering Research, Dindigul*, 1 (3), 518-527.
- Amer, S. M., Morsy, M. A., Hussein. M. A., Atlam, A & Mosa E. S. (2015). Effect of welding parameters variation on the weldability of austenitic stainless steel 304L, *International Journal of Scientific and Engineering Research*, 6 (2), 589-595.
- American Standard for Testing and Measurement ASTM E 8 – 04 (2011). Standard Test Method for Microindentation Hardness of Materials, ASTM International. West Conshohocken, www.astm.org
- American Standard for Testing and Measurement ASTM E3-11(2011). Standard Guide for Preparation of Metallographic Specimens, ASTM International, West Conshohocken, www.astm.org
- Arivarasu M., Devendranath R. K. & Arivazhagan, N. (2015). Characterization of tensile strength and impact toughness of autogenous PCGTA weldments of aeronautical steel and austenitic stainless steel, *Kovove Mater*, 54, 279–288.
- Arpita, N. B. & Vikram, A. P. (2016). Influence of process parameters of TIG welding process on mechanical properties of 304LSS welded joint, *International Research Journal of Engineering and Technology*, 3, 977.
- Behnam, S., Hassan, S., Mahdi, R., Ahmad Reza. A. & Ehsan, S. (2019). Microstructural, mechanical and corrosion properties of dissimilar joint between AISI A321 stainless steel and ASTM A537CL1 structural steel produced by GTAW process, *Metall. Res. Technol.*, 116 (4), 145-157
- Bhatti, A. R., Saggese, M. E., Hawkins, D. N., Whiteman, J. A. & Golding, M. S. (1984). Analysis of inclusions in submerged arc welds in micro alloyed steels, *Welding Journal*, 63 (7), 224-230.
- Çalik, A. (2009). Effect of cooling rate on hardness and microstructure of AISI 1020, AISI 1040 and AISI 1060 steels, *Int. J. of Phys. Sci*, 4 (9), 514-518.
- Devakumar, D. & Jabaraj, D. B. (2014). Research on gas tungsten arc welding of stainless steel – An overview, *International Journal of Scientific and Engineering Research*, 5 (1), 1612–1618.
- Ghuseen, R. M., Mahadzir, I., Syarifah, N. A. & Hassan A. A. (2017). Effects of heat input on microstructure, corrosion and mechanical characteristics of welded austenitic and duplex stainless steels, *A Review, Metals*, 7 (39), 123-136.
- Gigović-Gekić, A., Oruč, M. & Gojić, M. (2011). Determination of the content of delta ferrite in austenitic stainless steel nitronic 60, in Proceedings of 15th International Research/Expert Conference, Prague, Czech Republic, 157-160.
- Halil Ibrahim, K. & Ramazan, S. (2003). Study on microstructure, tensile test and hardness 304 stainless steel jointed by TIG welding, *International Journal of Science and Technology*, 2 (2), 163-168.
- Hansen, N. (2004). Hall–Petch relation and boundary strengthening, *Scr Mater*, 51, 801–806.
- Hayes, J. R., Gray, J. J., Szmodis, A. W. & Orme, C. A. (2006). Influence of chromium and molybdenum on the corrosion of nickel-based alloys. *Corrosion*, 62, 491-500.
- Hussain, A. K (2010): Influence of welding speed on tensile strength of welded joint in TIG welding process, *International Journal of Applied Engineering Resources*, 518.
- Hussein, M. & Fawzia, K. (2013). Mechanical and microstructure properties of 304 stainless steel friction welded joint, *International Research Journal of Engineering Science, Technology and Innovation (IRJESTI)* 2 (4), 65-74.
- Kondapalli, S. P., Ch.Srinivasa, R. D. & Nageswara, R.(2011). Optimizing Fusion Zone Grain Size and Ultimate Tensile Strength of Pulsed Current Micro Plasma Arc Welding Welded SS304L Sheets Using Hooke and Jeeves Algorithm, Proceedings of International Conference on Futuristic Trends in Materials and Energy Systems, V R Siddhartha Engineering College, Vijayawada, A.P., India, 112-119
- Kožuh, S., Gojić, M. & Kosec, L. (2009). Mechanical properties and microstructure of austenitic stainless steel after welding and post-weld heat treatment, *Kovove Mater*. 47, 253–262.
- Kutelu, B. J., Adubi, E. G. & Seidu S. O. (2018). Effects of electrode types on the microstructure, tensile and hardness properties of 304 L austenitic stainless steel heat-affected zone (HAZ), *Journal of Minerals and Materials Characterization and Engineering*, 6, 32-38.
- Laura, L., Leonel, D., Abreu, C., Brasil, M. & Pedro, B. (2019). Corrosion behavior of austenitic stainless steel welds prepared by dual protection GTAW process in 0.5 M H₂SO₄ and 3.5%wt. NaCl, *Int. J. Electrochem. Sci.*, 14, 1007-10092, www.electrochemsci.org
- Lippold, J. C. & Kotecki, D. J. (2005). Welding metallurgy and weldability of stainless steels.
- Mohamed, H.F., Firas, N.Q., Mohammed, A. & Jawda, A.(2024). Influence of welding current on mechanical and microstructure of argon arc welding of type- 304L austenitic stainless steel, *International Review of Mechanical Engineering (IREME)*, 18(4), <https://doi.org/10.15866/ireme.v/i424369>

- Mohd, S., Mohd, F. & Hasan, P.K.B. (2014). Effect of welding speed, current and voltage on mechanical properties of underwater welded mild steel specimen (C, Mn, Si) with Insulated Electrode E6013, *MIT International Journal of Mechanical Engineering*, 4 (2), 120-124.
- Ogundimu, E. O., Akinlabi, E. T. & Erinosh, M. F. (2019). Effect of welding current on mechanical properties and microstructure of TIG welding of ty-304 austenitic stainless steel, *Journal of Physics: Conference Series*, 1375(3),
- Okonji, P. O., Ulu, O. A. & Ubido, O. (2019). Effect of welding current on the hardness of austenitic stainless steels joints, *World Engineering and Applied Journal*, 10(2), 65-69. DOI: 10.5829/idosi, weasj.
- Oyetunji, O., Kutelu, B. J. & Akinola, A. S. (2013). Effects of welding speeds and power inputs on the hardness property of type 304 austenitic stainless steel heat-affected zone (HAZ), *Journal of Metallurgical Engineering (ME)*, 2 I, 124-129.
- Pauli, L., Jani, R., Heikki, R. & Teemu, S. (2016). Characterization of local grain size variation of welded structural steel, *Weld World*, 60, 673-688.
- Schmuki, P., Hildebrand, H., Friedrich, A. & Virtanen, S. (2005). The composition of the boundary region of MnS inclusions in stainless steel and its relevance in triggering pitting corrosion. *Corros Sci.*, 47, 1239-1250.
- Soon-Hyeok, J., Do. H. H., Hye-Jin., K. & Yong-Soo. P. (2014). Influence of oxygen content on the inclusion formation and pitting corrosion resistance of hyper duplex stainless steels, *Materials Transactions*, 55 (3), 1872 – 1877.
- Tabish, T. A., Abbas T., Farhan, M., Atiq, S. & Butt, T. Z. (2014). Effect of heat input on microstructure and mechanical properties of the TIG welded joints of AISI 304 stainless steel, *International Journal of Scientific and Engineering Research*, 5, 2014 – 1532.
- Thewlis, C. & Milner D. R. (1977). Inclusion formation in arc welding, *Welding Research Supplement*, 281-288.
- Vinoth. V., Madhavan. R. & Tharanitharan. G. (2015). Investigation on property relationship in various austenitic stainless steel 304L welds, *International Journal of Scientific and Research Publications*, 5 (3), 2250 -3153
- Wan Shaiful, H. W., Muda1, N. M. & Saifulnizan, J. (2015). Effect of welding heat input on microstructure and mechanical properties at coarse grain heat affected zone of ABS Grade A Steel, *ARNP Journal of Engineering and Applied Sciences*, 10 (20), 9487-9495.
- Wichan, C. & Loeshpahn, S. (2013). Effect of welding speed on microstructures, mechanical properties and corrosion behavior of GTA welded AISI 201 stainless steel sheets, *Journal of Materials Processing Technology*, 214, 402-408.
- Woel-Shyan, L., Fan-Tzeng. M. & Chi-Feng., L. (2005). Mechanical properties of 304L stainless steel SMAW joints under dynamic impact loading, *Journal of Materials Science*, 40 (3), 439-484.
- Zakaria, B., Chemseddine, D. & Thierry, B. (2010). Effect of welding on microstructure and mechanical properties of an industrial low carbon steel, *Scientific Research Engineering*, 2 502 - 506 doi:10.4236/eng.2010.27066
Published Online
(<http://www.SciRP.org/journal/eng>)